Atmos. Chem. Phys., 11, 705–721, 2011
www.atmos-chem-phys.net/11/705/2011/
doi:10.5194/acp-11-705-2011

Atmospheric Chemistry and Physics

Assessment of fossil fuel carbon dioxide and other anthropogenic trace gas emissions from airborne measurements over Sacramento, California in spring 2009

J. C. Turnbull[1,2], **A. Karion**[1,3], **M. L. Fischer**[4], **I. Faloona**[5], **T. Guilderson**[6], **S. J. Lehman**[2], **B. R. Miller**[1,3], **J. B. Miller**[1,3], **S. Montzka**[1], **T. Sherwood**[7], **S. Saripalli**[7], **C. Sweeney**[1,3], **and P. P. Tans**[1]

[1]National Oceanic and Atmospheric Administration, Earth Systems Research Laboratory, 325 Broadway, Boulder, CO 80305, USA
[2]Institute of Alpine and Arctic Research, University of Colorado at Boulder, Boulder, CO 80309-0450, USA
[3]Cooperative Institute for Research in Environmental Sciences, University of Colorado at Boulder, Boulder, CO 80309-0216, USA
[4]Lawrence Berkeley Laboratory, 1 Cyclotron Rd, Berkeley, CA 94720, USA
[5]Dept. of Land, Air and Water Resources, University of California, Davis, CA 95616-8627, USA
[6]Lawrence Livermore National Laboratories, Center for Accelerator Mass Spectrometry, Livermore, CA 94551, USA
[7]KalScott Engineering, 811 E 28th St, Lawrence, KS 66046, USA

Received: 26 August 2010 – Published in Atmos. Chem. Phys. Discuss.: 10 September 2010
Revised: 28 December 2010 – Accepted: 10 January 2011 – Published: 25 January 2011

Abstract. Direct quantification of fossil fuel CO_2 (CO_2ff) in atmospheric samples can be used to examine several carbon cycle and air quality questions. We collected in situ CO_2, CO, and CH_4 measurements and flask samples in the boundary layer and free troposphere over Sacramento, California, USA, during two aircraft flights over and downwind of this urban area during spring of 2009. The flask samples were analyzed for $\Delta^{14}CO_2$ and CO_2 to determine the recently added CO_2ff mole fraction. A suite of greenhouse and other trace gases, including hydrocarbons and halocarbons, were measured in the same samples. Strong correlations were observed between CO_2ff and numerous trace gases associated with urban emissions. From these correlations we estimate emission ratios between CO_2ff and these species, and compare these with bottom-up inventory-derived estimates. Recent county level inventory estimates for carbon monoxide (CO) and benzene from the California Air Resources Board CEPAM database are in good agreement with our measured emission ratios, whereas older emissions inventories appear to overestimate emissions of these gases by a factor of two. For most other trace species, there are substantial differences (200–500%) between our measured emission ratios and those derived from available emission inventories. For the first flight, we combine in situ CO measurements with the measured CO:CO_2ff emission ratio of 14 ± 2 ppbCO/ppmCO_2 to derive an estimate of CO_2ff mole fraction throughout this flight, and also estimate the biospheric CO_2 mixing ratio (CO_2bio) from the difference of total and fossil CO_2. The resulting CO_2bio varies dramatically from up to 8 ± 2 ppm in the urban plume to -6 ± 1 ppm in the surrounding boundary layer air. Finally, we use the in situ estimates of CO_2ff mole fraction to infer total fossil fuel CO_2 emissions from the Sacramento region, using a mass balance approach. The resulting emissions are uncertain to within a factor of two due to uncertainties in wind speed and boundary layer height. Nevertheless, this first attempt to estimate urban-scale CO_2ff from atmospheric radiocarbon measurements shows that CO_2ff can be used to verify and improve emission inventories for many poorly known anthropogenic species, separate biospheric CO_2, and indicates the potential to constrain CO_2ff emissions if transport uncertainties are reduced.

Correspondence to: J. C. Turnbull
(jocelyn.turnbull@noaa.gov)

Published by Copernicus Publications on behalf of the European Geosciences Union.

1 Introduction

Accurate quantification of anthropogenic trace gas emissions is needed to improve our understanding of their impacts on climate, ecosystems, and human health, and is essential for assessing whether emission control regulations are met (Pacala et al., 2010). Current knowledge of emissions for most anthropogenic gases is primarily based on bottom-up inventories obtained by tabulating the estimates of emissions from individual known sources or sectors. Due to incomplete identification or inaccurate assessment of multiple potential sources and their spatial and temporal variability, the uncertainties in these inventories are challenging to quantify. Fossil fuel CO_2 (CO_2ff) emissions are arguably the best known of the anthropogenic gases, as the carbon content of fossil fuels is well known, and fossil fuel usage is well documented through economic data for some parts of the world. At the national, annual scale in North America and Western Europe, uncertainties in CO_2ff emissions are as small as 3–5% (Boden et al., 2009), but uncertainties increase at smaller spatial and temporal scales, and, at the urban scale, may be 50–100% (Gurney et al., 2009; Peylin et al., 2009). Uncertainties for other gases emitted during combustion are generally much larger because their emissions are usually calculated from fuel use, using estimated emission factors (amount of the gas released per unit of fuel used), which can vary dramatically depending on the fuel type and combustion conditions. For example, carbon monoxide (CO) is produced during incomplete combustion, and the emission ratio of CO to CO_2ff (R_{CO/CO_2ff}) varies from 0.1 to 100 ppbCO/ppmCO_2ff, with the lowest values being associated with large, efficient power plants, and larger values observed from vehicles and domestic coal burning (e.g. Ohara et al., 2007; USEPA, 2009). Recent efforts to improve air quality have also resulted in a decrease in CO emissions from anthropogenic sources over the last decade (Hudman et al., 2008; Parrish et al., 2006; Warneke et al., 2006). For other gases emitted in the same urban area, such as halocarbons and industrial chemicals, even when production rates are well known, the rate and location of leakage to the atmosphere depends on a number of factors (e.g. TEAP, 2006; McCulloch et al., 2003). Relating them to CO_2ff in the urban area could help improve estimates of their emissions.

At the global scale, top-down atmospheric quantification of total emissions of long-lived gases is relatively straightforward, depending only on accurate measurements at remote locations (e.g. TEAP, 2006; Pozzer et al., 2010; Pacala et al., 2010). In particular, "top-down" atmospheric observations of trace gases can constrain CO_2 exchange, though continental to global scale studies have often used emission inventories to prescribe CO_2ff emissions to obtain estimates of biosphere fluxes (e.g. Gurney et al., 2002). Increasingly, there is interest in quantifying emissions at finer spatial scales (e.g., nation, province, state, county, city), for both regulatory and scientific purposes. At regional to national scales, atmospheric transport plays a decisive role in affecting measured mixing ratios and hence reconstruction of atmospheric transport is essential for determining regional emissions using inverse models (e.g. Zhao et al., 2009; Stephens et al., 2007; Gerbig et al., 2003; Gurney et al., 2002).

Accurate determinations of recently added CO_2ff mole fraction (here defined as CO_2ff enhancement in the boundary layer relative to the overlying free troposphere) can be used to constrain top-down estimates of trace gas emissions, both directly and by correlation. First, improved understanding of both fossil fuel CO_2 emissions and CO_2 exchange due to natural biogeochemical cycling (biosphere and oceans) is needed. When the CO_2ff component can be isolated, then the remaining CO_2 variability over continental regions (where there is no ocean CO_2 flux) can be ascribed to terrestrial biosphere CO_2 exchange and/or biomass burning. Secondly, when emissions of CO_2ff and another long-lived trace gas are co-located at the scale of interest, and the emission flux of CO_2ff is known, the measured ratio (R_{tracer/CO_2ff}) of the two gases can be used to determine the emissions of the trace gas. As long as the source region is approximately known, both gases are sufficiently long-lived in the atmosphere, and the emissions of both species are large enough to be distinguished from the background mole fraction, then uncertainties due to atmospheric transport are minimized. While the CO_2ff flux is not perfectly known, the fractional uncertainty in CO_2 emission is often small compared to that of other trace gases. Finally, atmospheric observations of CO_2ff can be used to infer the CO_2ff emissions flux, if atmospheric transport can be adequately described.

Here, we present observations of CO_2ff mole fraction inferred from observations of $\Delta^{14}CO_2$ and a suite of trace gas species from two aircraft flights conducted eight days apart in spring of 2009 over Sacramento, California, USA. Sacramento is a medium sized city (1.4 million inhabitants in the metropolitan region). There is little heavy industry in the city, although there are a number of oil refineries along the shipping channel to the southwest. The landscape of the surrounding region is dominated by agriculture. Our flights were both made during northwesterly wind conditions, and the flights were planned to sample the urban plume downwind of the urban region.

Measurements of $\Delta^{14}CO_2$ are used to directly constrain the CO_2ff mole fraction in flask samples in Sect. 3.1. We then use the flask measurements of CO_2ff and other trace gas species to identify the urban signature of the observed plume in Sects. 3.2 and 3.3. We also consider the implications of using total CO_2 enhancement as a proxy for CO_2ff. In Sect. 3.4, we compare the trace gas observations with bottom up emission inventories. In Sect. 3.5, we combine the $\Delta^{14}CO_2$-derived estimates of the CO_2ff mole fraction with in situ observations of CO to obtain an in situ record of CO_2ff during one flight and partition the observed CO_2 into CO_2ff and CO_2bio components. Finally, in Sect. 3.6, we use the in situ CO_2ff record to estimate the CO_2ff emission

flux from the Sacramento urban area, using a mass balance approach. Comparison with bottom-up inventory information allows assessment of uncertainties in this observationally based estimate of CO_2ff emissions.

2 Methods

2.1 Sample collection

Two flights were made over the Sacramento region, on 27 February 2009 (SAC227) and 6 March 2009 (SAC306), as part of a larger two-week campaign to measure greenhouse gases over the Sacramento and San Francisco Bay regions. Each of the two Sacramento flights began by flying north from the Napa Airport, ascending to ∼3000 m above sea level (m a.s.l.) to obtain representative free tropospheric background samples, then descended again to capture the boundary layer signal at 300–400 m a.s.l. (surface altitude is 0–25 m a.s.l. for this region), flying a zigzag path over and downwind of Sacramento (Fig. 1). Each downwind leg of the flight crossed the entire urban plume, capturing some "background" boundary layer air outside the urban plume at the ends of each leg. The aircraft then flew over the Walnut Grove tower (WGC, 38.3° N, 121.5° W; instrumented with in situ CO_2 and CH_4 and daily flask samples which are also analyzed at NOAA), where it made a pass by the tower at low altitude and spiraled up into the free troposphere before returning to Napa Airport. Both flights were about three hours long, beginning at around 02:00 p.m. local time (22:00 UTC). The winds were from the northwest for both flights, with wind speeds of 1–2 m s^{-1}.

In situ measurements of CO_2 were made using a Picarro CRDS flight-ready $CO_2/CH_4/H_2O$ analyzer (model G1301-m, unit CFADS30; Crosson, 2008; Chen et al., 2010). The analyzer pulled air from a wing-mounted inlet continuously at 300 sccm and measured both gases at 0.5 Hz. Reference tanks were sampled for 1.5 min every 15 to 20 min. Three standard reference gas tanks were used, calibrated at NOAA/ESRL on the WMO standard scale with CO_2 mole fractions ranging from 358 to 415 ppm (Zhao and Tans, 2006). For SAC227, the analyzer was deployed with an instrumentation box upstream that dried and pressure-controlled the sample, but which was found to be ineffective under very humid conditions and removed prior to the SAC306 flight. The CO_2 data were corrected for water vapor post-flight using a correction that was determined in the laboratory using the same analyzer unit. The CO_2 water correction is consistent to within 0.1 ppm with the manufacturer's correction and with the correction used by Chen et al. (2010) for the same analyzer type. Corrections were typically 0.3 ppm for SAC227 and 5 ppm for SAC306. The resulting water-corrected data was then further corrected using a linear calibration performed in the laboratory with five standard tanks prior to the campaign, and then by a single

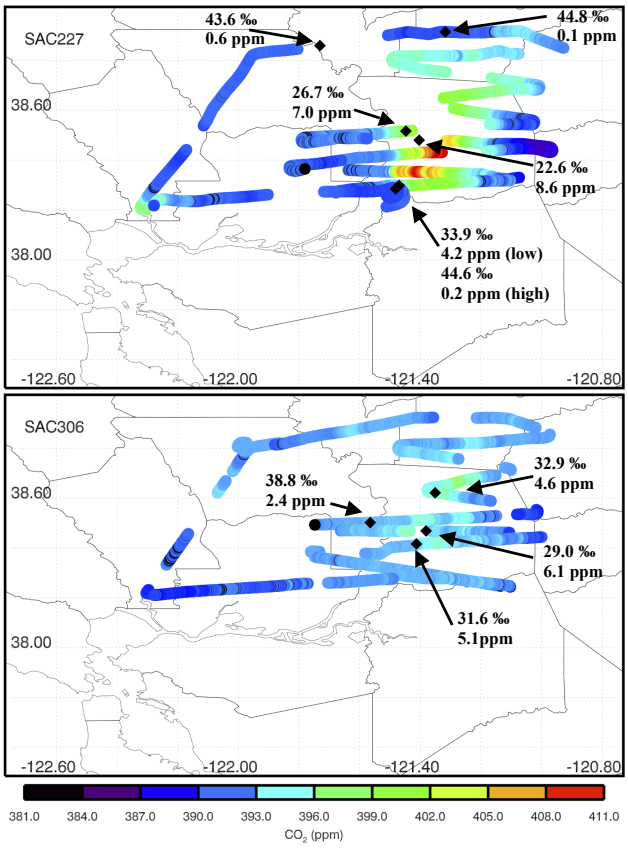

Fig. 1. Flight paths and CO_2 mole fraction (ppm) measured in situ during two flights above Sacramento on 27 February 2009 (SAC227, top) and 6 March 2009 (SAC306, bottom). Black diamonds indicate the locations where flask samples were collected. Measured $\Delta^{14}CO_2$ and calculated recently added CO_2ff mole fraction are indicated for each flask. One-sigma uncertainties are 0.2 ppm for in situ CO_2, 2.5‰ for $\Delta^{14}CO_2$ and ∼1 ppm for CO_2ff (see text). County and continent boundaries are shown for reference.

offset using the value of the first in-flight reference tank, linearly interpolated with time. The remaining two tanks were treated as unknowns for the purpose of quality control. Overall uncertainty of the in situ CO_2 measurement (including the water correction) is estimated as 0.2 ppm. A more detailed description of the in situ analyzer system will be reported by Karion et al. (2011).

The CO measurements were made with a commercial instrument manufactured by Aero-Laser (model AL5002). The instrument drew approximately 200 sccm of ambient air from a second wing mounted inlet, passing it through a Nafion dryer, and detecting CO by vacuum-UV resonance fluorescence (Gerbig et al., 1999). At approximately 40 min intervals during each flight, a calibration gas prepared by Scott Specialty was used to track the instrument sensitivity. A chemical scrubber was used to create a zero mole fraction sample for determining the instrument blank. The signal

noise appeared to be Poisson in nature with a one-sigma precision of 2.9 ppb in one second at typical ambient conditions. Cross calibration with a NOAA certified CO cylinder indicated agreement to within 1–2% of ambient concentrations.

Programmable Flask Packages (PFPs) were used to collect 4–6 discrete flask sample pairs during each flight. To obtain sufficient sample for $\Delta^{14}CO_2$ measurement, two flasks were collected at each sampling location and time. Typically the two flasks were flushed and filled in parallel over a period of approximately two minutes, with almost all of the air in each flask coming from the last ∼20 s. The first flask of each pair was measured for CO_2, CO, CH_4, SF_6, H_2, N_2O, a suite of hydrocarbons and halocarbons, and stable isotopes of CO_2 (both ^{13}C and ^{18}O) using methods documented online (http://www.esrl.noaa.gov/gmd/ccgg/aircraft/index.html), and by Montzka et al. (1993) and Vaughn et al. (2004). The remaining air in this flask was combined with all air in the second flask for a single $\Delta^{14}CO_2$ measurement, obtaining about 0.4–0.5 mgC from each sample.

For the two flights described, we compared in situ CO_2 and CO data with the flask data. For SAC227, four of six flasks overlapped with in situ data; the mean offset (in situ minus flask) was -0.05 ± 0.14 ppm CO_2, and -6.7 ± 5 ppb for CO. For SAC306, five flasks were compared with a mean offset of -0.12 ± 0.2 ppm for CO_2. Offsets were greater when flasks were sampled during periods of high variability in concentration, likely due to some uncertainty in the time synchronization and real atmospheric variability during flask filling.

2.2 $\Delta^{14}CO_2$ measurements

High precision $\Delta^{14}CO_2$ measurements were made by: (a) extracting the CO_2 from whole air, using a newly developed automated extraction system at the University of Colorado INSTAAR Laboratory for AMS Radiocarbon Preparation and Research (NSRL) (Turnbull et al., 2010); (b) graphitizing the samples by reaction with hydrogen over iron catalyst with magnesium perchlorate to remove water at the Center for Accelerator Mass Spectrometry (CAMS) (Graven et al., 2007); and (c) high count accelerator mass spectrometer (AMS) ^{14}C measurement at CAMS using a method slightly modified from Graven et al. (2007). The methods are similar to those described by Turnbull et al. (2007) but utilizing a new extraction system and a different AMS system, which differs slightly in both measurement technique and performance.

Measurement uncertainties are assessed by analysis of repeat extraction aliquots of whole air from high pressure cylinders. The extraction procedure is the same as for authentic flask samples, and there is no discernable bias between flask and cylinder extraction. For the present work, three different surveillance cylinders were used, identified as NWT_{std}, NWT3, and NWT4. NWT_{std} contains ambient air collected at Niwot Ridge, Colorado in late 2002 and has been used extensively to quantify uncertainties in $^{14}CO_2$ measurements at NSRL (Turnbull et al., 2007; Lehman et al., 2010). NWT3 and NWT4 are newly prepared tanks designed to replace NWT_{std}, which is near exhaustion. NWT3 contains ambient air collected at Niwot Ridge in 2009. NWT4 is similar, but spiked with ^{14}C-free CO_2 to produce a slightly lower $\Delta^{14}CO_2$ value.

NBS Oxalic Acid I (OxI) was used as the primary measurement standard, and was prepared entirely at CAMS following their standard procedures. NBS Oxalic Acid II (OxII) was measured as an additional secondary standard, with some being prepared at CAMS, and others prepared to CO_2 gas stage at NSRL. The process blank was determined in extraction aliquots from a high pressure cylinder of synthetic ^{14}C-free air at NSRL. This serves primarily as a screen for possible ^{14}C contamination during preparation and measurement.

This dataset was collected in three separate "wheels" (measurement runs) over a period of three consecutive days. Each target was measured to a total of ∼1 000 000 ^{14}C counts. The measurement protocol differed slightly from that described by Graven et al. (2007) in that the number of targets (including authentic samples and standards) in each wheel was increased from 24 to 40, taking ∼24 h to measure each wheel. Individual measurement wheels consisted of eight OxI primary measurement standards, one process blank, 10 surveillance targets (four NWT_{std}, three NWT3, three NWT4), four OxII secondary measurement standards, and 17-20 authentic samples. Including eight primary standards (versus the six typically used by Graven et al., 2007) reduces potential wheel-to-wheel biases due to a single outlier standard target. Wheel-to-wheel differences in AMS tuning can affect the measured values, so the larger wheel size with more samples can reduce overall measurement uncertainty by reducing the number of wheels.

The mean measurement value and one-sigma measurement repeatability (across all three AMS runs) for each of the surveillance materials and for OxII are given in Table 1. The pooled standard deviation of all surveillance materials is 2.5‰. Within each wheel, the pooled standard deviation is smaller, at 1.8‰. The precision for this first set of samples measured by NSRL/CAMS was slightly poorer than is typical for CAMS, and appears to be related to the particular AMS tuning and target conformation for these measurements, and not due to the larger wheel size. We report the $\Delta^{14}CO_2$ uncertainty as the larger value of 2.5‰. This uncertainty is applied to both sample and background $\Delta^{14}CO_2$ values, resulting in an uncertainty of 1.3 ppm in CO_2ff. For reference, a 1 ppm CO_2ff signal decreases $\Delta^{14}CO_2$ by ∼2.6‰.

The surveillance material results agree well with measurements of the same materials prepared at NSRL and measured using the University of California, Irvine AMS (Table 1).

Table 1. Mean $\Delta^{14}C$ values of secondary standard materials measured at CAMS for this experiment, and long-term measurements made at UCI since 2002. Values are reported as the mean and one-sigma repeatability of each dataset, with the number of measured targets given in brackets.

	LLNL	UCI	Difference
OxII	340.1 ± 1.7 (6)	339.3 ± 2.7 (178)	0.7 ± 0.7
NWT_{std}	73.6 ± 2.6 (12)	73.9 ± 1.9 (325)	-0.3 ± 0.7
NWT3	41.6 ± 3.5 (9)	42.4 ± 1.5 (24)	-0.9 ± 1.2
NWT4	-32.8 ± 2.3 (9)	-31.9 ± 1.3 (23)	-1.0 ± 0.8

3 Results and discussion

3.1 Calculation of CO_2ff in flask samples

The CO_2ff mole fraction in each flask sample was calculated from the measured $\Delta^{14}CO_2$ value and CO_2 mole fraction in each flask, such that

$$CO_{2_{ff}} = \frac{CO_{2_{obs}}\left(\Delta_{obs} - \Delta_{bg}\right)}{\Delta_{ff} - \Delta_{bg}} - \frac{CO_{2_{other}}\left(\Delta_{other} - \Delta_{bg}\right)}{\Delta_{ff} - \Delta_{bg}} \quad (1)$$

where Δ_{obs} is the $\Delta^{14}CO_2$ value in each sample, and $CO_{2_{obs}}$ is the observed CO_2 mole fraction in the same sample. Δ_{ff} is, by definition, -1000‰ (zero ^{14}C content). Δ_{bg} is the background $\Delta^{14}CO_2$ value. The second term of the equation is a small correction for the effect of other sources of CO_2 which have a $\Delta^{14}C$ value differing from that of the atmosphere. $CO_{2_{other}}$ is the added mole fraction from these other sources (principally heterotrophic respiration, and also including CO_2 from biomass burning), and Δ_{other} is the average $\Delta^{14}C$ value of these sources. We estimate this correction as -0.2 ± 0.1 ppm (the correction is subtracted, hence increasing CO_2ff) for samples collected at this location and time of year (Turnbull et al., 2006, 2009).

Δ_{bg} was selected from the flask containing the lowest CO mixing ratio (113.45 ppb), which was collected in SAC227 in the free troposphere at the end of the flight. All species measured in this sample confirm that this is a reasonable choice of background sample, with most hydrocarbon and halocarbon species exhibiting low values, a CO_2 mixing ratio 389.04 ppm, and, as expected, a high $\Delta^{14}CO_2$ value of 44.6 ± 2.5‰ (the addition of ^{14}C-free CO_2ff works to reduce the $\Delta^{14}CO_2$ value). The $\Delta^{14}CO_2$ value in this sample is not distinguishable from the two other free troposphere samples in these flights (44.8 ± 2.5‰ and 43.6 ± 2.5‰), nor from free troposphere samples collected in four other flights made in the California Central Valley region during the same two-week period (data not shown). All the free troposphere samples exhibit $\Delta^{14}CO_2$ values higher than those taken in the boundary layer. We also considered using a Δ_{bg} value from a continental background site such as Niwot Ridge, Colorado (Turnbull et al., 2007). Two Niwot Ridge measurements spanning the same time period (17 February to 17 March 2009) have $\Delta^{14}CO_2$ values ranging from 44.5 ± 1.8‰ to 46.2 ± 1.8‰, in agreement with our chosen background value. We include an uncertainty of 1.0‰ in Δ_{bg}, estimated from the spread of the free troposphere and Niwot Ridge samples. The resulting CO_2ff values have an uncertainty of 1.0–1.3 ppm at one-sigma. We note also that any bias in the choice of $\Delta^{14}CO_2$ background is consistent throughout the dataset and thus will not influence our correlations with other trace gases or the determination of emission ratios, because in those cases, it is the slope, and not the intercept, that matters (Sects. 3.2, 3.3 and 3.4).

The $\Delta^{14}CO_2$ and calculated CO_2ff values vary substantially throughout the flights (Fig. 1). The samples taken in the boundary layer, and within the urban plume, all have $\Delta^{14}CO_2$ values lower than the free troposphere samples, indicating the addition of ^{14}C-free CO_2ff from the urban area. The values range from 38.8 ± 2.5‰ to 22.6 ± 2.5‰ in $\Delta^{14}CO_2$ and 2.4 ± 1.0 to 8.6 ± 1.0 ppm CO_2ff, providing signals that are significantly above our detection limit for CO_2ff. The sample taken at 400 m a.s.l. over the Walnut Grove tower in this flight had a $\Delta^{14}CO_2$ value of 33.9 ± 2.5‰ (4.2 ± 1.0 ppm CO_2ff), similar to the 36.5 ± 2.5‰ (3.2 ± 1.0 ppm CO_2ff) value for a sample taken at 91 m at the tower two hours earlier.

3.2 Emission ratio for CO

The ^{14}C-derived CO_2ff values in each flask were correlated with the suite of additional trace gas species measured in the same samples. In this section, we discuss the comparison with the CO measurements in detail, and the following section covers the remaining species.

The correlation between CO_2ff and CO is strong ($r^2 = 0.96$), and consistent across both flights (Fig. 2). CO emissions are associated with combustion sources (both anthropogenic and natural), but also have a large source from oxidation of volatile organic compounds (VOCs), especially in summer (Bergamaschi et al., 2000). Although the CO atmospheric lifetime of about two months at this latitude and time of year (Spivakovsky et al., 2000) is short compared to the CO_2 lifetime, removal of CO is negligible in this case, because the samples were collected within a day of emission from the source region (maximum flight distance from Sacramento is ~50 km, and wind speed was 1–2 m s^{-1}, Mesinger et al., 2006, http://www.emc.ncep.noaa.gov/mmb/rreanl/). As we discuss later, emissions from surrounding counties may also contribute to the observed CO_2ff and CO, and these emissions also would have occurred within a day or so of emission.

We calculated the observed emission ratio of CO to CO_2ff (R_{CO/CO_2ff}) using a linear regression of the correlation between CO and CO_2ff (Fig. 2, Table 2). The regression

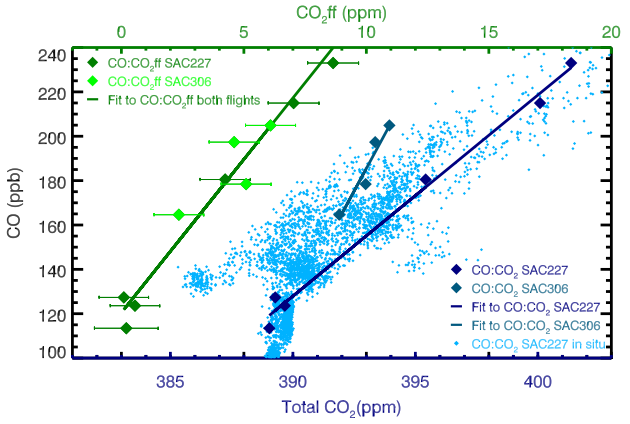

Fig. 2. Correlations between measured CO and CO_2ff and between measured CO and total CO_2. Flask measurements of CO:CO_2ff are shown in green, using the top x-axis. CO:CO_2 correlations (flasks and in situ) are shown in blue, using the bottom x-axis. Error bars are the one-sigma uncertainty in CO_2ff; uncertainties in CO and CO_2 are smaller than the symbol size. Fitted lines are linear regressions with errors in both coordinates.

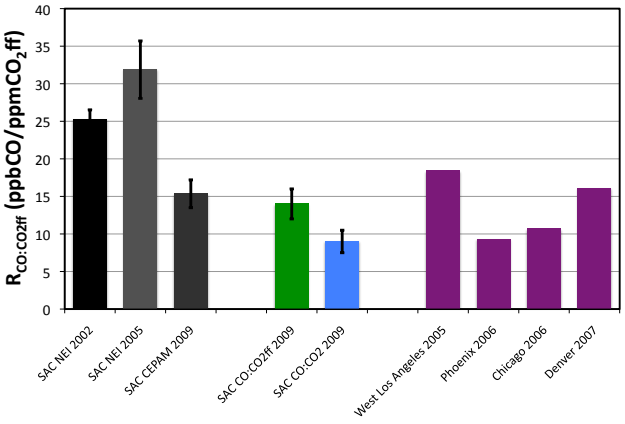

Fig. 3. CO:CO_2ff emission ratios. Gray bars: inventory based emission ratios, from CO and CO_2ff inventories. CO inventories are from the USEPA NEI database for 2002 and 2005 and California Air Resources Board CEPAM database for 2009. The emission ratio is calculated from each CO inventory using two CO_2ff inventories (Vulcan and CEPAM), extrapolated to the same year as the CO inventory. Error bars are derived from the difference between the two CO_2ff inventories. Green: R_{CO/CO_2ff} from this study. Blue: R_{CO/CO_2} from this study (using total CO_2 rather than CO_2ff). Purple: direct on-road tailpipe emission measurements from Bishop and Stedman (2008).

includes the uncertainties in both coordinates (Press and Teukolsky, 1992), which are typically 1.0 ppm in CO_2ff and 2 ppb in CO. The R_{CO/CO_2ff} value is 14 ± 2 ppb/ppm for both flights combined (coefficient of determination $r^2 = 0.96$), and no significant difference is seen if R_{CO/CO_2ff} is calculated separately for each flight, although the correlation is slightly weaker ($r^2 = 0.7$) for the four flasks from SAC306 flight alone. We also tested the possibility that the free troposphere samples might be influenced by different sources (and background) and therefore impact the calculated emission ratio. Excluding the three free troposphere samples resulted in R_{CO/CO_2ff} of 12 ± 3 ppb ($r^2 = 0.90$), not significantly different from that calculated including the free troposphere samples. Our empirical determination of R_{CO/CO_2ff} falls within the range of R_{CO/CO_2ff} measurements made by direct measurement of vehicle tailpipe emissions of CO and CO_2 in several other US cities (Fig. 3) including West Los Angeles (18.4 ppb/ppm in 2005), Chicago (10.7 ppb/ppm in 2006), Phoenix (9.3 ppb/ppm in 2006) and Denver (16.1 ppb/ppm in 2007) (Bishop and Stedman, 2008).

In contrast to CO_2ff, we also determined the ratio of CO to *total* CO_2, here designated R_{CO/CO_2}. When we calculate R_{CO/CO_2} for our dataset, we obtain R_{CO/CO_2} of 9 ± 1 ppb/ppm for both flights combined (vs. R_{CO/CO_2ff} of 14 ± 2 ppb/ppm, Figs. 2 and 3). Unlike R_{CO/CO_2ff}, the measured R_{CO/CO_2} values differ by a factor of two between the two flights, with values of 9.0 ± 0.4 and 20 ± 4 ppb/ppm for SAC227 and SAC306 flights, respectively. The in situ CO and CO_2 measurements from SAC227 give R_{CO/CO_2} of 9 ppb/ppm, roughly consistent with the flask-based R_{CO/CO_2} from the same flight, but also differing from R_{CO/CO_2ff}. These results suggest that there are contributions to CO_2 variability from other sources, such as biospheric CO_2 exchange and biomass combustion, including biofuel use, in the enhancement (or depletion) of total CO_2. In our study, the non-fossil contribution apparently varies substantially, and changes sign, between the two measurement dates. We discuss this further in Sect. 3.5. It follows that care should be taken in interpreting emission ratios based on CO_2 mole fraction alone (R_{CO/CO_2}), as they may be substantially biased.

3.3 Emission ratios of other trace gas species

Numerous species associated with combustion sources, anthropogenic activity and biomass burning were measured in the same flask samples analyzed for $\Delta^{14}CO_2$. A total of ten samples were measured for $\Delta^{14}CO_2$, but unfortunately, instrument problems meant that two of the four flasks from SAC306 were not measured for many of these additional species, and so some correlations are for eight measurement pairs only (six from SAC227 and two from SAC306).

Hydrocarbon species that are associated with anthropogenic sources (benzene, acetylene, propane, isopentane and n-pentane), as well as total pentanes (isopentane plus n-pentane) show very strong correlations with CO_2ff, with the coefficient of determination (r^2) ranging from 0.9–1.0 (Fig. 5, Table 2). These correlations are robust even when the three free troposphere samples are excluded from the analysis. While benzene and acetylene are associated with anthropogenic combustion sources and with biomass burning,

Table 2. Inventory-based and observed $R_{\text{tracer}/CO_2\text{ff}}$. Emission ratios for CO and CH_4 are reported in ppb/ppm, all others are reported in ppt/ppm. Inventory estimates are calculated using the CEPAM CO_2ff inventory (low value) and Vulcan CO_2ff inventory (high value). Observed values are calculated from the slope of the relationship between each tracer and CO_2ff, along with one-sigma uncertainties and coefficient of determination of those slopes. For species where the slope differed significantly when the two flights were considered individually, or when the free troposphere samples were excluded from the fit, the slope is also given for those subsets.

Species	NEI 2005 gridded	EDGAR 2005 gridded	NEI 2002 SAC Co	CARB 2008 SAC Co	**Observed 2009**	**Coefficient of determination (r^2)**
Fossil fuel sources						
Carbon monoxide[1]	32–36		25–28	15–17[2]	**14±2**	**0.96**
Boundary layer samples only					*12±3*	*0.90*
SAC227 only					*14±2*	*0.99*
SAC306 only					*14±6*	*0.70*
Benzene	27–30		26–29	14–16	**15±2**	**0.89**
Acetylene	35–39				**52±7**	**0.97**
Isopentane					**64±8**	**0.95**
n-pentane					**18±2**	**0.99**
Pentanes[3]	234–262				**82±10**	**0.96**
Propane	30–34				**109±17**	**0.81**
Boundary layer samples only					*64±18*	*0.55*
Industrial solvents						
Dichloromethane			8.4–9.4	6.2–6.9	**4±1**	**0.62**
Boundary layer samples only					–	*0.03*
Perchloroethylene			6.3–7.1		**1.4±0.2**	**0.91**
Chloroform				0.1–0.1	**2.0±1.2**	**0.93**
Carbon tetrachloride				0.001	–	**0.20**
Biomass burning/ocean source						
Methyl bromide			1.2–1.4	1.2–1.4	–	**0.28**
Methyl chloride			0.04	0.04	–	**0.37**
Carbonyl sulfide			0.001	0.002	–	**0.46**
Dielectric insulator						
Sulphur hexafluoride		1.8–2			**0.2±0.1**	**0.19**
SAC227 only					*0.03±0.01*	*0.45*
SAC306 only					*0.10±0.05*	*0.81*
Halocarbons						
HFC-152a		3.1–3.4			**9±1**	**0.92**
HFC-143a		2.5–2.7			**0.9±0.1**	**0.88**
HFC-134a		12–13			**4±1**	**0.96**
HFC-125		1.4–1.6			**0.6±0.1**	**0.86**
HCFC-142b		2.0–2.2			**0.3±0.1**	**0.89**
HCFC-22					**7±1**	**0.92**
Multiple sources						
Methane					**15±2**	**0.89**
Boundary layer samples only					*11±4*	*0.72*
SAC227 only					*15±3*	*0.93*
SAC306 only					*7±4*	*0.71*
Nitrous oxide					**0.21±0.04**	**0.74**
SAC227 only					*0.20±0.03*	*0.89*
SAC306 only					*−0.1±0.1*	*0.39*

[1] also sourced from biomass burning and VOCs;

[2] calculated for 2009, see text;

[3] includes both i- and n-pentanes.

propane, isopentane and n-pentane are strongly associated with vehicular emissions and evaporation of fuel from vehicles and fueling stations as well as refineries (Watson et al., 2001; Baker et al., 2008). The very strong correlations between CO_2ff and these species suggest that the observed CO_2ff is due in large part to vehicles, consistent with expectations for an urban region.

A suite of halocarbons and solvents that are currently in use in industrial and commercial applications also show very strong correlations with CO_2ff ($r^2 = 0.85$–0.96, Fig. 5, Table 2). HFC-134a (1,1,1,2-tetrafluoroethane) is used in mobile (vehicle) air conditioners and home refrigerators, and shows the strongest correlation (highest r^2) with CO_2ff. HCFC-22 (chlorodifluoromethane, used in building air conditioning), HFC-152a (difluoroethane, aerosol propellant used in air dusters and deodorants), HFC-125 (pentafluoroethane, refrigerant used in supermarket cooling), chloroform and perchloroethylene (industrial solvents) also show significant positive correlations with CO_2ff. This provides further confirmation that the observed plume is from the urban region.

Conversely, tracers associated with other types of sources do not have statistically significant correlations with CO_2ff in our samples (Fig. 5, Table 2). Methyl chloride and methyl bromide are emitted from biomass burning, and also have significant ocean and natural vegetative sources, and the lack of enhancement in these species in the plume indicates an absence of biomass burning influence from our measurements. The slight negative relationship between methyl chloride and CO_2ff (Fig. 5) is consistent with a strong surface-related sink for methyl chloride. Halocarbons that are being phased out (CFC-11, CFC-12) do not correlate with CO_2ff in our measurements, suggesting very low or no emissions.

Sulphur hexafluoride (SF_6) enhancements vary dramatically between the two flights. For SAC306, SF_6 is enhanced in all the samples, and correlates quite well to CO_2ff ($r^2 = 0.81$), but almost no correlation is seen in SAC227 (Fig. 5, Table 2). SF_6 is entirely anthropogenic and used to quench sparks in electrical facilities, and is extremely stable in the troposphere (Geller et al., 1997). Although it has been suggested as a potential proxy for CO_2ff (e.g. Rivier et al., 2006; Potosnak et al., 1999; Bakwin et al., 1998; Wofsy et al., 1994), atmospheric measurements suggest that the point source nature of SF_6 results in a variable SF_6:CO_2ff emission ratio (R_{SF_6/CO_2ff}), especially at small scales (Turnbull et al., 2006). Our results indicate that although R_{CO/CO_2ff} appears homogenous for our two measurement dates, R_{SF_6/CO_2ff} is not, perhaps because SF_6 comes from only a few localized point sources within the urban region, and/or those emissions might be episodic.

Methane (CH_4) and nitrous oxide (N_2O) are both produced during combustion, but also have numerous biological sources, including a large source from cattle and dairy farms (Bousquet et al., 2006; Hirsch et al., 2006), both of which are common in the California Central Valley. Both species correlate strongly with CO_2ff in our samples ($r^2 = 0.89$ for CH_4 and $r^2 = 0.74$ for N_2O, Fig. 5, Table 2). However, the regression slopes are likely to be influenced by contributions from sources other than combustion, in particular, dairy farming and wetlands in the region. These two species also show some differences between the two flights, with strong correlations in SAC227, and weaker correlations in SAC306, suggesting that there are subtle differences in the source region, background values and/or emissions for the two flights. Further discussion of the CH_4 and N_2O measurements is the focus of a forthcoming companion paper by Karion et al.

3.4 Comparison of measured emission ratios with inventory data

Currently, most information about anthropogenic trace gas emissions is determined from bottom-up inventories, whereby emissions from all known sources are tallied to obtain total emissions for a given region and time period. It is difficult to ascertain the uncertainty of these inventories, as numerous factors contribute to total uncertainty (IPCC, 2000). Generally, emissions of CO_2ff are assumed to be better quantified in inventory data than those of other species including CO, especially at large scales, because the usage and carbon content of fossil fuels are relatively well known. At the annual, national level, uncertainties in CO_2ff are 3–5% (Pacala et al., 2010). At the county scale in California, comparisons of CO_2ff from two different (albeit not completely independent) inventories suggest somewhat larger uncertainties of at least 10–20% (de la Rue du Can, private communication). For many other species, including CO, emissions are calculated from fossil fuel use, using an estimated emission factor for each individual source or source type, and uncertainties are difficult to quantify (Frey and Small, 2003).

We now compare our atmospheric observations with the bottom-up inventory data, recognizing that our observations are from only two mid-afternoon flights in February/March, and the available inventory data is usually annual averages. In order to make this comparison, we must first estimate the source region influencing sampled air. Based on the plume location (Fig. 1) and back-trajectories obtained from the HYSplit model (Draxler and Rolph, 2010) we approximate the region of influence as Sacramento County, which includes all of the Sacramento metropolitan area.

We use several different inventory datasets. For CO_2ff, we use the Vulcan inventory for Sacramento County (Gurney et al., 2009). The Vulcan inventory is available only for 2002, so we assume a 1.1% yr^{-1} increase in CO_2ff (CEPAM database, http://www.arb.ca.gov/ei/ei.htm) and extrapolate the Vulcan CO_2ff value to 2009. The Vulcan CO_2ff estimate for Sacramento County is 2.8 MtC yr^{-1} for 2002, and the 2009 extrapolated value is 3.0 MtC yr^{-1}. The California Air Resources Board CEPAM database also inventories CO_2ff emissions. The most recent available estimate for Sacramento County is 2.5 MtC yr^{-1} for 2004 (S. de la

Rue de la Can, personal communication, 2010), which we extrapolate to 2.6 MtC yr^{-1} in 2009. The difference between the Vulcan and CEPAM inventories is likely larger than the uncertainty related to the extrapolation procedure. For each inventory-based emission ratio, we calculate the emission ratio using both Vulcan and CEPAM CO_2ff; with the CEPAM value resulting in the higher emission ratio estimates shown in Table 2.

The US Environmental Protection Agency NEI database (http://www.epa.gov/ttn/chief/eiinformation.html) provides county level CO emissions inventories. However, the latest available NEI county level data is for 2002, and extrapolation of the preceding years' estimates to 2009 would result in a zero value for CO emissions (Fig. 4). Instead, we do not extrapolate, but use the 2002 NEI CO value (and the Vulcan CO_2ff estimate for 2002) to calculate a NEI/Vulcan 2002 R_{CO/CO_2ff} value of 25–28 ppb/ppm, somewhat higher than our observationally-based estimate (Table 2, Fig. 3). A more recent gridded ($0.1° \times 0.1°$) NEI CO inventory is available for 2005, but is for July averages only (Frost et al., 2005). We therefore extract the annual CO emissions for a gridbox approximating Sacramento County (38.2–38.7° N, 121.0–121.6° W) and assume flat emission throughout the year. We also extract Vulcan CO_2 emissions for the same gridded region and extrapolate them to 2005. We obtain NEI/Vulcan 2005 R_{CO/CO_2ff} of 32–36 ppb/ppm, which is substantially higher than the county level estimate (Table 2, Fig. 3). We also obtain an estimate of CO emissions from the California Air Resources Board CEPAM database (http://www.arb.ca.gov/ei/ei.htm) by applying an exponential fit to extrapolate the 5 yearly inventory estimates (Fig. 4). The exponential fit was chosen, as it is gives an extremely good fit ($r^2 = 0.99$) to the 1995–2010 CEPAM values. This gives a CEPAM/Vulcan 2009 R_{CO/CO_2ff} value of 15–17 ppb/ppm for 2009, the same year as our measurements (Table 2, Fig. 3). This is in agreement with our atmospheric observation of 14 ± 2 ppb/ppm, but we note that our measurement is for only two afternoons during the year, versus the inventory data which are averaged over the entire year. The agreement with our empirical observations does not rule out a possible bias in both the CO and CO_2ff inventories, especially since the two inventories are not entirely independent, with a small component of the Vulcan CO_2ff inventory (area emissions) being derived from CO inventories (Gurney et al., 2009) and vice versa (USEPA, 2001). In addition, seasonal variations of the emissions ratio around the annual mean may influence the comparison. Our results are nevertheless consistent with several studies which have shown that the NEI inventories are a factor of two too high at several locations in the US (Graven et al., 2009; Hudman et al., 2008; Parrish et al., 2006; Turnbull et al., 2006; Warneke et al., 2006), and suggest that the CEPAM CO inventory is a substantial improvement over the older bottom-up CO emission inventories.

We also compare the observed benzene:CO_2ff ratio with ratios derived from inventory data. As the benzene inventory

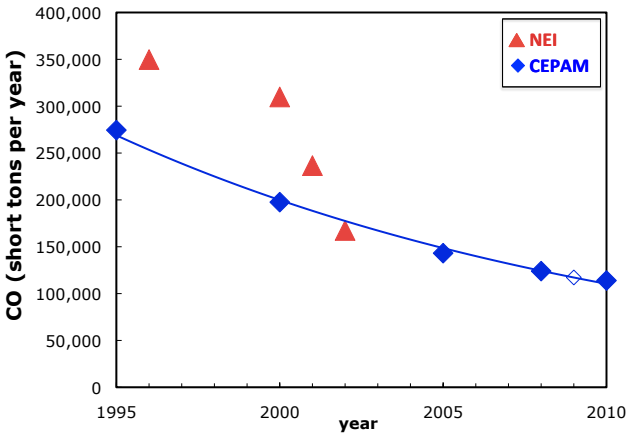

Fig. 4. Inventory-based estimates of CO emissions for Sacramento County, California. Red points are from USEPA NEI county level database (http://www.epa.gov/ttn/chief/eiinformation.html). Solid blue points are from the California Air Resources Board CEPAM database (http://www.arb.ca.gov/ei/ei.htm). The open blue point is interpolated for 2009 from the fitted curve (blue line) to the CEPAM datapoints.

data is sparser than for CO, and we cannot accurately determine a trend, we use the most recent inventory data available from each source without extrapolation. As for the CO results, we find good agreement between our observations from the two flights with the annual benzene emission ratio estimate from the 2008 CEPAM inventory for Sacramento County (using CO_2ff from Vulcan and CEPAM for 2008), whereas the two NEI inventories for 2002 and 2005 overestimate the observed values by about a factor of two (Table 2, Fig. 6). For the other hydrocarbon species (acetylene, the pentanes and propane), the most recent and most detailed inventory is the NEI July 2005 gridded dataset. This inventory underestimates the acetylene and propane emissions we derive from ratios to CO_2ff by a factor of 2–3, and overestimates pentane emissions (Table 2). We also compare emission ratios for other atmospheric measurements made in Los Angeles in 2002, and Boston and New York in 2004 (Warneke et al., 2007) and from Boston and New York between 1999–2005 (Baker et al., 2008). These emissions ratios are reported with respect to CO rather than CO_2ff. For the purposes of comparison with our data and with the inventories, we convert their $R_{tracer/CO}$ ratios to R_{tracer/CO_2ff}, assuming $R_{CO/CO_2ff} = 14$ ppb/ppm. The measured emission ratios vary by about 50% across the different urban areas and time periods, likely due to differences in fuel mix, temperature and combustion efficiencies. Despite these differences between the observations, and the short time period over which our observations were made, all of the observations tend to be broadly consistent, whereas we see differences between the inventories and observations of 200–500% for many of the species (Fig. 6). The benzene inventories are

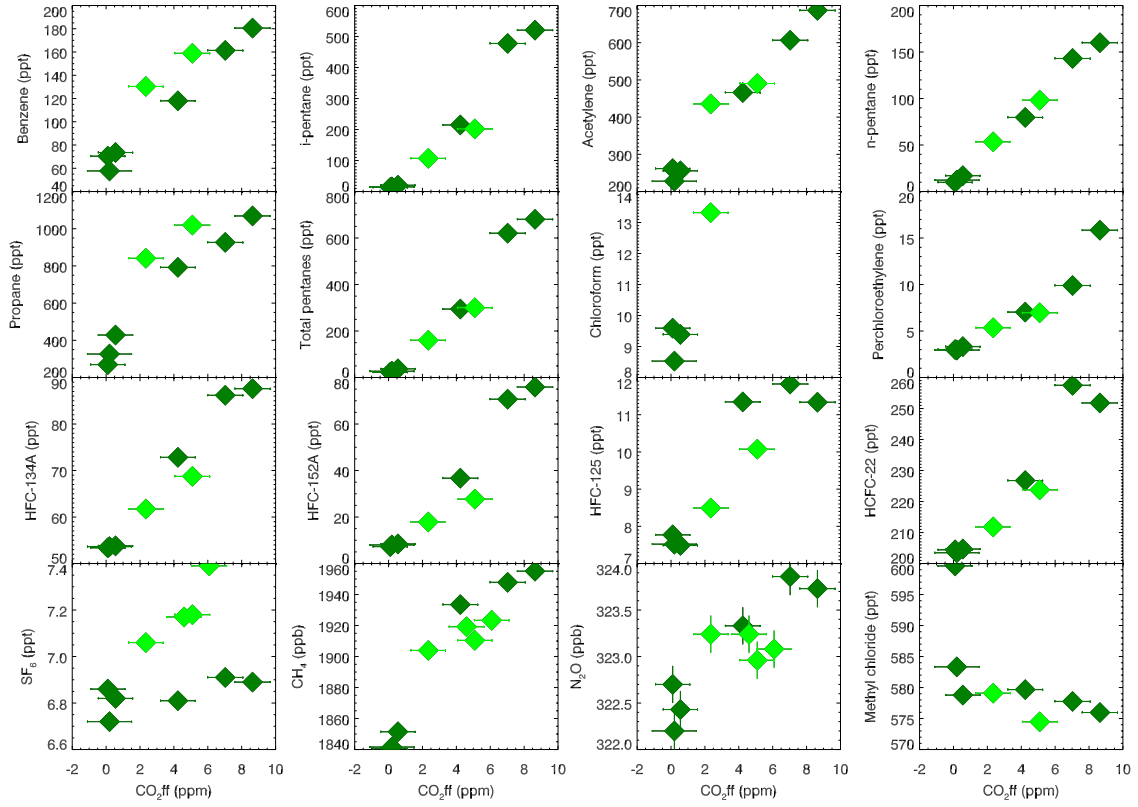

Fig. 5. Correlations between CO_2ff and selected species measured in the same flasks. Dark and light green symbols are flasks from SAC227 and SAC306, respectively. Lines are the linear regression with errors in both coordinates for flasks from both flights combined. Errors on the y-axis are often smaller than the symbol size.

most consistent with the observations, whereas the inventories for acetylene and propane are consistently lower than the observations. The pentane inventories are consistently higher than the observations, although this may be biased by the shorter atmospheric lifetime of the pentanes (Atkinson et al., 2007).

The observed emission ratios for the industrial solvents dichloromethane and perchloroethylene are lower than the inventory data. The chloroform emissions are substantially higher than the inventories, which may be related to the potentially large natural sources of chloroform. With such a small dataset and no additional observations for comparison, it is difficult to further assess the source of the differences between inventories and observations.

For the halocarbon species and SF_6, no county level data is available. Instead, we extract estimates from the EDGAR v4 2005 gridded emission inventory (EDGAR, 2009), the same gridded region as for the NEI 2005 gridded inventory. The gridded EDGAR emissions are for the most part obtained by disaggregating country level emissions, rather than on fine-scale bottom-up inventories. We find that the observations and inventories typically agree within a factor of three, quite reasonable given the uncertainty in the inventory at the urban scale of our observations, and the potential temporal bias in the comparison of our small observational dataset and the annual inventories. The exceptions are SF_6 and HCFC-142b, for which the observed emissions are an order of magnitude smaller than the inventory values. HCFC-142b is being phased out, so lower emissions than the 2005 inventories might be expected, although there is as yet no other atmospheric data to support this observation. SF_6 emissions are associated with leaks at electrical facilities, and the spatial and temporal pattern of these may be very different than the spatial allocation used in the EDGAR database.

3.5 In situ CO_2ff and CO_2bio

CO measurements can potentially be used to determine CO_2ff at lower cost and higher resolution than is currently possible with $\Delta^{14}CO_2$ measurements alone, if R_{CO/CO_2ff} can be accurately determined. Levin and Karstens (2007) and Vogel et al. (2010) have demonstrated the feasibility of using $\Delta^{14}CO_2$ and CO measurements in flasks to determine R_{CO/CO_2ff} for a particular location and time period, and then applied this R_{CO/CO_2ff} to in situ CO measurements to obtain a high resolution CO_2ff record (here designated as CO_2ff^{CO}).

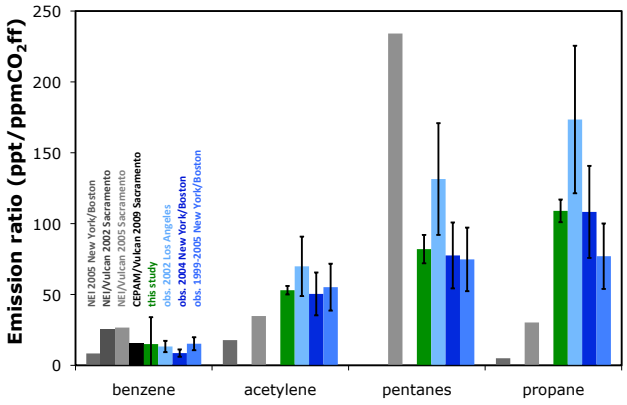

Fig. 6. Hydrocarbon emission ratios from inventories and observations. For each species, up to four inventory estimates are shown in grays, and are (from left to right): New York/Boston NEI 1999 inventory, Sacramento NEI/Vulcan 2002 inventory, Sacramento NEI/Vulcan 2005 inventory, Sacramento CEPAM/Vulcan 2009 inventory. Observation-based estimates from this study are shown in green. Three blue bars are (from left to right) observations from Los Angeles in 2002, Boston/New York in 2004 (Warneke et al., 2007), and Boston/New York in 1993–2005 (Baker et al., 2008).

CO_2ff^{CO} is calculated as

$$CO_2ff^{CO} = \frac{CO_{obs} - CO_{bg}}{R_{CO/CO_2ff}} \quad (2)$$

where CO_{obs} is the observed CO mole fraction, and CO_{bg} is a background CO value. We use in situ (two second) observations of CO from SAC227 (Fig. 7), and a CO_{bg} value of 113 ppb, obtained from the free troposphere flask samples, described in Sect. 3.1. Unfortunately, no in situ CO measurements were made during SAC306.

Uncertainties in CO_2ff^{CO} are dominated by the uncertainty in R_{CO/CO_2ff} and by the choice of CO_{bg}. We neglect the additional uncertainty and possible bias due to the influence of CO from sources other than fossil fuel combustion (e.g. open biomass burning, oxidation of hydrocarbons), as we have concluded that these sources are small for this dataset. The uncertainty in CO_2ff^{CO} due to uncertainty in R_{CO/CO_2ff} is about 15%, or 0.1 to 2 ppm, with the largest uncertainties when CO_2ff^{CO} is largest. The uncertainty in CO_{bg} is estimated as 10 ppb from the range of free troposphere measurements in both flasks and in situ measurements, contributing 0.7 ppm uncertainty to CO_2ff^{CO}. Thus when CO_2ff^{CO} is small, the uncertainty is dominated by the uncertainty in CO_{bg}, but when CO_2ff^{CO} is large, the uncertainty is dominated by the uncertainty in R_{CO/CO_2ff}. The resulting CO_2ff^{CO} values appear reasonable, with large values in the area over and downwind of Sacramento (Figs. 7 and 8), low values of ∼1 ppm CO_2ff in the boundary layer outside of the urban plume, and values indistinguishable from zero in the free troposphere.

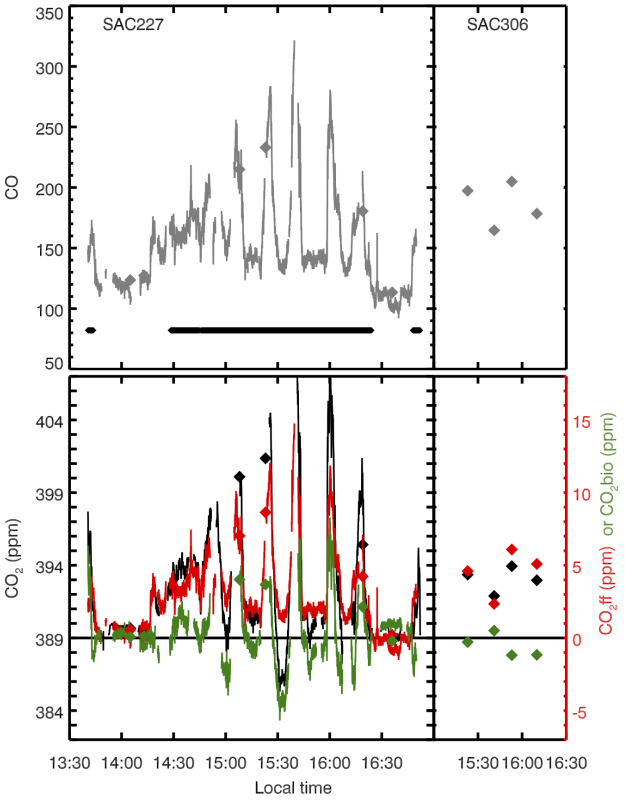

Fig. 7. Top panel: flask (diamonds) and in situ (lines) measurements of CO from SAC227 and SAC306. The black line indicates times when the aircraft was within the boundary layer. Bottom panel: flask (diamonds) and in situ (lines) measurements of: total CO_2 (black, left axis); CO_2ff^{CO} calculated from R_{CO/CO_2ff} and continuous CO (red, right axis); and CO_2bio calculated as the residual of total CO_2 and CO_2ff^{CO} (green). Uncertainties are 1 ppb in CO, 0.1 ppm in CO_2, 1 ppm in CO_2ff and CO_2bio from flasks, and 0.2–2 ppm in CO_2ff^{CO} and CO_2bio from in situ observations.

The contribution of CO_2bio can be calculated as the residual of the difference between total CO_2 and CO_2ff, such that

$$CO_2bio = CO_2obs - CO_2bg - CO_2ff \quad (3)$$

where CO_2obs is the observed CO_2 mole fraction in the flask or in situ measurement, CO_2bg is the background CO_2 value, and CO_2ff is from either $\Delta^{14}CO_2$ measurements (for flasks) or from CO_2ff^{CO}. The contribution of CO_2 from ocean exchange is assumed to be zero, since the measurements are made over land, and any ocean contribution is effectively included in CO_2bg. We use CO_2bg of 389.0 ppm, the value measured in the same flask used for Δ_{bg} and CO_{bg}, and assign an uncertainty of 0.3 ppm to this value, based on the range of flask and in situ free troposphere CO_2 measurements. We calculate CO_2bio for the SAC227 in situ measurements, and for the flasks in both flights. The uncertainty in CO_2bio ranges from 0.4 to 2 ppm.

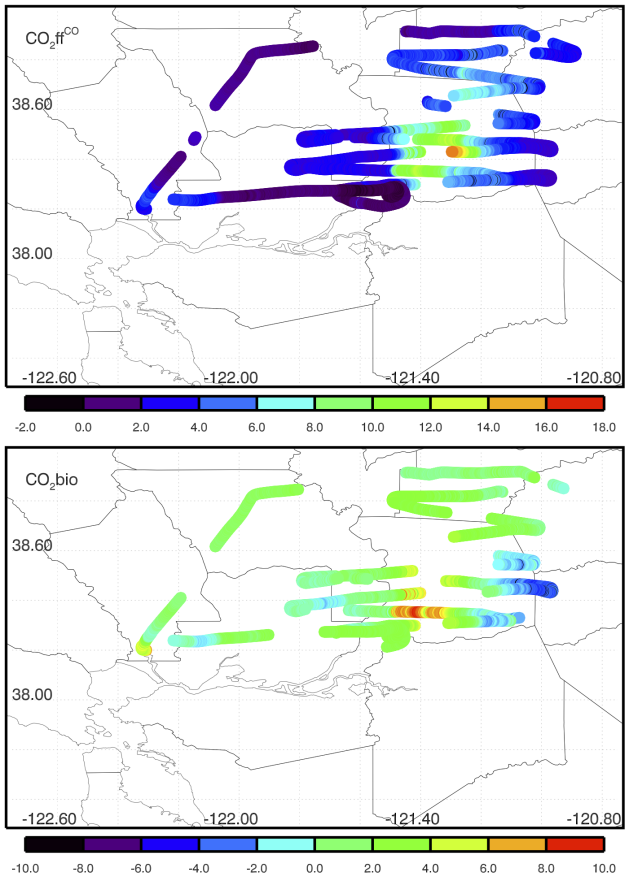

Fig. 8. Continuous CO_2ff (top) and CO_2bio (bottom) for SAC227 shown as a function of flight path. Units are ppm.

The in situ measurements show large peaks in CO_2 mole fraction over and downwind of Sacramento. While CO_2ff makes up most of the CO_2 enhancement in these peaks, it is not sufficient to explain the entire enhancement (Figs. 7 and 8). We considered the possibility that CO_2ff was underestimated, but it is difficult to explain the required underestimate of up to 6 ppm in CO_2ff (17‰ in $\Delta^{14}CO_2$), by biases such as the choice of Δ_{bg}, CO_{bg} and measurement uncertainty, which we estimate equates to an uncertainty of 0.2 to 2 ppm. Thus a positive contribution of up to 8 ppm to the CO_2 enhancement over the urban region on February 27 is apparently from CO_2bio. Conversely, in the rural areas outside the urban plume, CO_2bio is negative, with a minimum of −6 ppm CO_2bio. Positive biosphere contributions could be from above and below ground respiration, biofuel use such as in liquid fuels, anthropogenic combustion of biomass such as for home heating, or forest fires and other open biomass burning. Photosynthesis has a negative contribution to CO_2bio.

Low temperature biomass combustion (e.g. wood fires) is unlikely to contribute to CO_2bio in SAC227 as the high CO:CO_2 ratio expected from this source (40–70 ppb/ppm, Andreae and Merlet, 2001) is not observed, because air temperatures were 14–20 °C (i.e. warm enough that home heating from wood fires is not likely), and because no enhancements occur in either methyl chloride or methyl bromide (Fig. 5), both of which are produced during biomass burning (Andreae and Merlet, 2001).

Use of biofuels likely contributes up to 1 ppm of the positive CO_2bio signal, as California required ∼8% ethanol in gasoline in 2009 (CARB, 2008), and this ethanol is usually derived from biological sources. Differences in vegetation between the urban and surrounding rural areas may explain the remaining difference in CO_2bio, with the rural areas dominated by agriculture and grasslands, whereas trees are more dominant in the urban area, especially since our measurements are in the spring, when biomes are transitioning from a net CO_2 source to a net sink. In the SAC306 flask samples, we find that CO_2bio is close to zero inside the urban plume (Fig. 7), suggesting that a substantial bias in our CO_2ff or CO_2bio calculations (e.g. due to our choice of background CO and CO_2 values) is an unlikely explanation for the large CO_2bio values inside the plume from SAC227.

The near-zero CO_2bio values inside the urban plume from SAC306 also indicate a weaker respiration/biofuel source and/or stronger photosynthetic uptake on this day. This observation is consistent with frontal activity that brought rain to the area between the dates of the two flights (California Air Resources Board AQMIS2 data archive, http://www.arb.ca.gov/aqmis2/metselect.php), which may have resulted in differing CO_2bio fluxes on the two flight dates.

3.6 Estimate of the CO_2ff flux

In Sects. 3.2 and 3.3, we reported emission ratios of various trace gas species to CO_2ff, making the case that CO_2ff emissions are likely the best known of any trace gas from inventories. Yet the uncertainty in CO_2ff from inventories is still significant, especially at the regional and urban scale. For California, the uncertainty in CO_2ff inventories at the county level is estimated to be at least 10–20% (S. de la Rue de la Can, personal communication, 2010). Atmospheric observations of CO_2ff can potentially be used to quantify these emissions, if the atmospheric transport is known.

We use a simple mass balance approach to estimate the CO_2ff flux from Sacramento County for flight SAC227. We carry out this estimate to demonstrate the utility of the approach, acknowledging that the large uncertainties reported here could be substantially reduced by incorporation of more detailed meteorological information. In this method, an aircraft flies transects across an emission plume, downwind of the source, in the boundary layer. The method was originally developed for trace gas emissions from point sources such as smokestacks, and here we apply it to the urban area source, implicitly treating the urban plume as a single well-mixed source. The measured mole fraction can be integrated

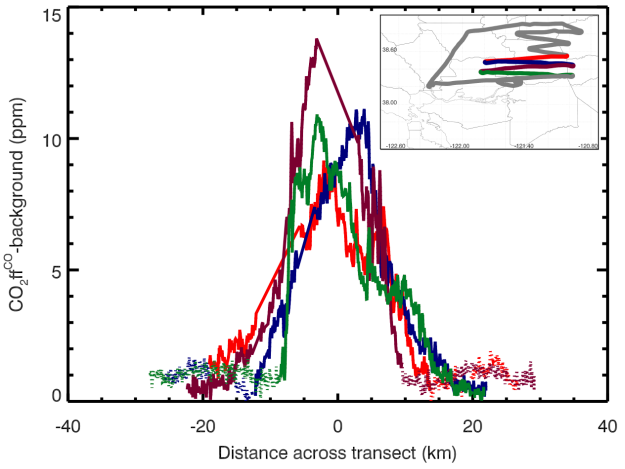

Fig. 9. X_{meas} (CO_2ff^{CO} – background CO_2) used to integrate for the flux calculation for each of four downwind transects in SAC227. Solid lines indicate the areas inside the plume for each transect. Inset, flight map showing the individual transects, with the same color coding.

to obtain a measure of the flux (Mays et al., 2009; Ryerson et al., 2001; Trainer et al., 1995; White et al., 1976):

$$\mathrm{flux} = v \cdot \cos\alpha \cdot \int_{\mathrm{gnd}}^{\mathrm{zPBL}} n(z)dz \cdot \int_{-y}^{y} X_{\mathrm{meas}}dy \qquad (4)$$

Flux is the total flux of CO_2ff in MtC yr^{-1}, from the emission area from which the plume is sourced. The source must be isolated, so that there are no overlapping plumes. We treat the Sacramento metropolitan area as the source of a single homogenous plume. The wind speed (v) is assumed to be constant through the time and space between the site of emission and the observation aircraft. The angle α between the aircraft track and the direction normal to the wind direction is here assumed to be zero. The number density of the atmosphere (n) is integrated vertically throughout the boundary layer, assuming that the plume is well-mixed in the vertical, and no leakage through the top of the boundary layer has occurred. The mole fraction enhancement over background (X_{meas}) is integrated across the entire horizontal span of the plume from location $-y$ to y. The boundary layer CO_2ff values outside the plume are elevated by about 1 ppm above the free troposphere measurements, indicating some CO_2ff is due to regional sources, and we subtract a mean boundary layer background of 0.95 ppm of CO_2ff from each CO_2ff^{CO} measurement to obtain X_{meas} at each point. This allows us to determine the flux contributing to the urban plume itself. We select the endpoints $-y$ and y subjectively from the shape of the plume for each transect (Fig. 9).

No meteorological measurements were made onboard the aircraft during this flight, and instead we use a variety of estimates for the boundary layer height, wind speed and wind direction. Wind direction was approximately 330°, consistent between the NARR reanalysis (horizontal resolution of 32 km and 3 hourly time step, Mesinger et al., 2006, http://www.emc.ncep.noaa.gov/mmb/rreanl/), measurements from the WGC tower at the same time, and the observed plume downwind of Sacramento urban area. The NARR reanalysis indicates that the wind speed over the city was 1.0 m s^{-1}, and increased to 1.7 m s^{-1} in the downwind plume. Measurements from the WGC tower, further downwind from our aircraft transects, indicate that the wind speed at 490 m ranged between 2.0 and 3.3 m s^{-1} during the same time period. We use the highest and lowest wind speed estimates as end members in our calculation. The NARR reanalysis estimates the boundary layer height as 1500 m, but is known to overestimate the boundary layer height in the California Central Valley. Instead, we directly estimated boundary layer height from the aircraft measurements of CO_2, CH_4, CO and temperature when the aircraft flew out of the boundary layer into the free troposphere. The boundary layer height from these observations appears much lower, at about 700 m, and is consistent with that obtained from a sounding over Oakland, California the same afternoon. We therefore use upper and lower boundary layer height estimates of 600 and 800 m in our calculations.

We calculate the flux independently for each of the four transects that were made in the downwind plume (Fig. 9, Table 3). For each transect we obtain a range of flux estimates calculated from the range of wind speeds and boundary layer heights. The mean flux estimate for Sacramento County from all four transects is 3.5 MtC yr^{-1}, with a range of 1.3–7.0 MtC yr^{-1}. Our observational estimate of CO_2ff flux during the afternoon of 27 February 2009 is comparable to the annual Vulcan and CEPAM estimates for Sacramento County (extrapolated to 2009) of 3.0 and 2.6 MtC yr^{-1}, respectively. Our observational estimate likely also includes some contribution from surrounding counties, which would bias it high relative to the inventory estimates. The large range of values in the observations estimate predominantly reflects the large uncertainty in wind speed and boundary layer height for this experiment. We also see a difference in flux estimates amongst the four transects, with the closer transects about 25% higher than the ones further downwind, which could be related to variability in wind speed during the experiment, or leakage out of the boundary layer that is not accounted for. The ∼100% uncertainty in this result is consistent with other studies using this mass balance method (Ryerson et al., 2001; Trainer et al., 1995).

4 Conclusions

This study demonstrates the utility of measurements of CO_2ff mole fraction in the atmosphere. Flask measurements of $\Delta^{14}CO_2$ allow us to directly constrain CO_2ff mole fractions and fluxes. The combination of flask CO and $\Delta^{14}CO_2$

Table 3. CO_2ff flux estimates for the Sacramento urban region from measurements made on 27 February 2009, and scaled to the annual total CO_2ff emissions, assuming constant emissions throughout the year. Transects are the four downwind flight segments shown in Fig. 9. Flux estimates for each transect are reported as the range of values using four different wind speed and boundary layer height estimates (see text). "Mean all observations" is the mean of all 16 realizations (four transects, four estimates each) of the calculations. Two bottom-up inventory estimates of the annual total emissions from Sacramento County from Vulcan (Gurney et al., 2009) and the California Air Resources Board CEPAM database (S. de la Rue de la Can, personal communication, 2010) are included for comparison.

	Annual total CO_2ff flux estimate (MtC yr^{-1})
Transect 1	1.6–7.0
Transect 2	1.4–6.2
Transect 3	1.3–5.7
Transect 4	1.3–5.6
Mean All Observational Flux Estimates	**3.5**
Vulcan	3.0
CEPAM	2.6

measurements with high-resolution CO measurements provides a method to estimate CO_2ff mole fractions at high resolution. Although the emission ratio of CO to CO_2ff is consistent across the measurements presented here, the emission ratio can be expected to vary for different locations and times. Therefore the emission ratio should be determined on a regular basis, either from every flight, or in the case of surface measurements, at regular time intervals.

Using $\Delta^{14}CO_2$ and CO measurements as a proxy for CO_2ff reveals structural detail in the distribution of CO_2ff and CO_2bio which cannot be obtained from CO_2 measurements alone. The enhancement in total CO_2 over Sacramento is largely due to CO_2ff, but also includes a significant contribution from CO_2bio (photosynthesis, respiration, and biomass combustion such as biofuel use), and the sign of the CO_2bio contribution varies within the urban plume even on dates only a week apart. The sign of the CO_2bio contribution is also seen to change within and outside the urban plume. If CO_2ff was approximated only by the total CO_2 enhancement, large and unpredictable biases in calculated emission ratios would have resulted.

The large suite of gases measured in flask samples permit us to identify the sources contributing to the observed CO_2ff plume. Strong correlations between CO_2ff and a suite of hydrocarbons indicate that much of the CO_2ff in the Sacramento plume comes from vehicle emissions. A suite of halocarbons associated with vehicle use and urban sources also correlate extremely well with CO_2ff. Conversely, gases associated only with biomass burning show no elevation in these samples. Gases associated with both combustion sources and agricultural sources show weaker and more variable correlations with CO_2ff.

Using an emission ratio approach, we compared our observation-based results from two flights in February and March 2009 with annual bottom-up inventory estimates for a host of trace gases. Recent annual, county level CEPAM emission inventories for CO and benzene agreed very well with our observations (despite the difference in temporal resolution of the observations and inventories), whereas older inventories appeared to overestimate emissions of these species by a factor of two; this conclusion is consistent with other recent atmospheric studies. For other hydrocarbon species, our results are broadly consistent with atmospheric observations of emissions from other US cities, whereas they often differ from inventory data. These discrepancies are likely due in part to the method of disaggregation of national level inventories to the regional scale. A larger observational dataset, collected over a longer time period and at varying times during the day, would be needed to confirm that the differences between the inventories and our observations are not an artifact of the particular sampling period.

Finally, we used a simple mass balance approach to demonstrate, albeit with observations from a single flight, that in situ CO_2ff observations, obtained from flask measurements of $\Delta^{14}CO_2$ and CO and in situ measurements of CO, can be used to quantify CO_2ff flux at the urban scale. In this initial study, where the experiment was not specifically designed to this end, and we did not collect meteorological data, we were able to estimate the CO_2ff flux with an uncertainty of $\sim$100%. Nevertheless, our estimated flux from this single flight agrees with annual bottom-up inventories within 20%. Improved measurement of wind speed and boundary layer height would dramatically improve the precision of this calculation. More sophisticated transport models, with resolution sufficient to evaluate transport at the urban scale, and which are able to account for changing meteorological conditions during the experiment (e.g. regional a transport model such as WRF) could also be used to improve the flux estimate. The uncertainty, as well as temporal variability, in the flux estimate could also be reduced by a larger suite of observations.

Acknowledgements. Aircraft infrastructure development and flight missions were supported by the Small Business Innovative Research program administered the US Department of Energy's Office of Biological and Environmental Research to Kalscott Engineering (Lawrence, KS) contract No. DE-FG02-04ER83986, and to the Lawrence Berkeley National Laboratory under contract No. DE-AC02-05CH11231. Thanks to Paula Zermeno for assistance and advice on $^{14}CO_2$ sample preparation. Two anonymous reviewers provided helpful feedback on an earlier draft of this paper.

Edited by: C. Gerbig

References

Andreae, M. O. and Merlet, P.: Emission of trace gases and aerosols from biomass burning, Global Biogeochem. Cy., 15, 955–966, 2001.

Atkinson, R., Arey, J., and Achmann, S. M.: Atmospheric chemistry of alkanes: Review and recent developments, Atmos. Environ., 42, 5859–5871, 2007.

Baker, A. K., Beyersdorf, A. J., Doezema, L. A., Katzenstein, A., Meinardi, S., Simpson, I. J., Blake, D. R., and Rowland, S.: Measurements of nonmethane hydrocarbons in 28 United States cities, Atmos. Environ., 42, 170–182, 2008.

Bakwin, P. S., Tans, P. P., White, J. W. C., and Andres, R. J.: Determination of the isotopic ($^{13}C/^{12}C$) discrimination by terrestrial biology from a global network of observations, Global Biogeochem. Cy., 12, 555–562, 1998.

Bergamaschi, P., Hein, R., Heimann, M., and Crutzen, P. J.: Inverse modeling of the global CO cycle 1. Inversion of CO mixing ratios, J. Geophys. Res., 105, 1909–1927, 2000.

Bishop, G. A. and Stedman, D. H.: A decade of on-road emissions measurements, Environ. Sci. Technol., 42, 1651–1656, 2008.

Boden, T. A., Marland, G., and Andres, R. J.: Global, regional and national fossil-fuel CO_2 emissions, Carbon Dioxide Information Analysis Center, Oak Ridge National Laboratory, US Department of Energy, Oak Ridge, Tenn., USA, 2009.

Bousquet, P., Ciais, P., Miller, J. B., Dlugokencky, E. J., Hauglustaine, D., Prigent, C., van der Werf, G. R., Peylin, P., Brunke, E.-G., Carouge, C., Langenfelds, R. L., Lathiere, J., Papa, F., Ramonet, M., Schmidt, M., Steele, L. P., Tyler, S. C., and White, J. W. C.: Contribution of anthropogenic and natural sources to atmospheric methane variability, Nature, 443, 439–443, doi:10.1038/nature05132, 2006.

Chen, H., Winderlich, J., Gerbig, C., Hoefer, A., Rella, C. W., Crosson, E. R., Van Pelt, A. D., Steinbach, J., Kolle, O., Beck, V., Daube, B. C., Gottlieb, E. W., Chow, V. Y., Santoni, G. W., and Wofsy, S. C.: High-accuracy continuous airborne measurements of greenhouse gases (CO_2 and CH_4) using the cavity ring-down spectroscopy (CRDS) technique, Atmos. Meas. Tech., 3, 375–386, doi:10.5194/amt-3-375-2010, 2010.

Crosson, E. R.: A cavity ring-down analyzer for measuring atmospheric levels of methane, carbon dioxide, and water vapor, Appl. Phys. B: Lasers and Optics, 92, 403–408, 2008.

Draxler, R. and Rolph, G.: HYSPLIT (HYbrid Single-Particle Lagrangian Integrated Trajectory) Model access via NOAA ARL READY Website (http://ready.arl.noaa.gov/HYSPLIT.php), 2010.

Frey, H. C. and Small, M. J.: Uncertainty in emission factors and emission inventories, J. Industrial Ecol., 7, 9–11, 2003.

Frost, G. J., McKeen, S. A., Trainer, M., Ryerson, T. B., Neuman, J., Roberts, J., Swanson, A., Holloway, J., Sueper, D., Fortin, T., Parrish, D. D., Fehsenfeld, F., Flocke, F., Peckham, S., Grell, G., Kowal, D., Cartwright, J., Auerbach, N., and Habermann, T.: Effects of changing power plant NOx emissions on ozone in the eastern United States: Proof of concept, J. Geophys. Res., 111, D12306, doi:10.1029/2005JD006354, 2006.

Geller, L. S., Elkins, J. W., Lobert, J. M., Clarke, A. D., Hurst, D. F., Butler, J. H., and Myers, R. C.: Tropospheric SF_6: Observed latitudinal distribution and trends, derived emissions and interhemispheric exchange time, Geophys. Res. Lett., 24, 675–678, 1997.

Gerbig, C., Schmitgen, S., Kley, D., Volz-Thomas, A., Dewey, K., and Haaks, D.: An improved fast-response vacuum-UV resonance fluorescence CO instrument, J. Geophys. Res., 104, 1699–1704, 1999.

Gerbig, C., Lin, J., Wofsy, S. C., Daube, B. C., Andrews, A. E., Stephens, B. B., Bakwin, P. S., and Grainger, C.: Toward constraining regional-scale fluxes of CO_2 with atmospheric observations over a continent: 2. Analysis of COBRA data using a receptor-oriented framework, J. Geophys. Res., 108, 4757, doi:10.1029/2003JD003770, 2003.

Graven, H. D., Guilderson, T. P., and Keeling, R. F.: Methods for high-precision ^{14}C AMS measurement of atmospheric CO_2 at LLNL, Radiocarbon, 49, 349–356, 2007.

Graven, H. D., Stephens, B. B., Guilderson, T. P., Campos, T. L., Schimel, D. S., Campbell, J. E., and Keeling, R. F.: Vertical profiles of biospheric and fossil fuel-derived CO_2 and fossil fuel CO_2 : CO ratios from airborne measurements of $\Delta^{14}C$, CO_2 and CO above Colorado, USA, Tellus, 61, 536–546, 2009.

Gurney, K. R., Law, R. M., Denning, A. S., Rayner, P. J., Baker, D., Bousquet, P., Bruhwiler, L., Chen, Y.-H., Ciais, P., Fan, S., Fung, I. Y., Gloor, M., Heimann, M., Higuchi, K., John, J., Maki, T., Maksyutov, S., Masarie, K. A., Peylin, P., Prather, M., Pak, B. C., Randerson, J., Sarmiento, J. L., Taguchi, S., Takahashi, T., and Yuen, C.-W.: Towards robust regional estimates of CO_2 sources and sinks using atmospheric transport models, Nature, 415, 626–630, 2002.

Gurney, K. R., Mendoza, D. L., Zhou, Y., Fischer, M. L., Miller, C. C., Geethakumar, S., and de la Rue du Can, S.: High resolution fossil fuel combustion CO_2 emission fluxes for the United States, Environ. Sci. Technol., 43, 5535–5541, doi:10.1021/es900806c, 2009.

Hirsch, A. I., Michalak, A. M., Bruhwiler, L. M., Peters, W., Dlugokencky, E. J., and Tans, P. P.: Inverse modeling estimates of the global nitrous oxide surface flux from 1998–2001, Global Biogeochem. Cy., 20, GB1008, doi:10.1029/2004GB002443, 2006.

Hudman, R., Murray, L., Jacob, D. J., Millet, D., Turquety, S., Wu, S., Blake, D. R., Goldstein, A., Holloway, J., and Sachse, G. W.: Biogenic versus anthropogenic sources of CO in the United States, Geophys. Res. Lett., 35, L04801, doi:10.1029/2007GL032393, 2008.

IPCC: Good practice guidance and uncertainty management in national greenhouse gas inventories, IPCC, 2000.

Karion, A.: Local signals of CO_2, CH_4 and N_2O in the San Francisco and Sacramento regions of California, in preparation, 2011.

Lehman, S. J., Miller, J. B., Turnbull, J. C., Southon, J. R., Tans, P. P., and Sweeney, C.: $^{14}CO_2$ measurements in the NOAA/ESRL Global Co-operative Sampling Network: An update on measurements and data quality, Expert Group Recommendations from the 15th WMO/IAEA Meeting of Experts on Carbon Dioxide, Other Greenhouse Gases and Related Tracer Measurement Techniques, Jena, 2010.

Levin, I. and Karstens, U.: Inferring high-resolution fossil fuel CO_2 records at continental sites from combined $^{14}CO_2$ and CO observations, Tellus, 59B, 245–250, 2007.

Mays, K. L., Shepson, P. B., Stirm, B. H., Karion, A., Sweeney, C., and Gurney, K. R.: Aircraft-based measurements of the carbon footprint of Indianapolis, Environ. Sci. Technol., 43, 7316–7823, 2009.

McCulloch, A., Midgley, P. M., and Ashford, P.: Releases of re-

frigerant gases (CFC-12, HCFC-22 and HFC-134a) to the atmosphere, Atmos. Environ., 37, 889–902, 2003.

Mesinger, F., DiMego, G., Kalnay, E., Mitchell, K., Shafran, P. C., Ebisuzaki, W., Jovic, D., Woollen, J., Rogers, E., Berbery, E. H., Ek, M. B., Fan, Y., Grumbine, R., Higgins, W., Li, H., Lin, Y., Manifin, G., Parrish, D. D., and Shi, W.: North American Regional reanalysis, B. Am. Meteorol. Soc., 87, 343–360, doi:10.1175/BAMS-87-3-343, 2006.

Montzka, S. A., Myers, R. C., Butler, J. H., Elkins, J. W., and Cummings, S.: Global tropospheric distribution and calibration scale of HCFC-22, Geophys. Res. Lett., 20, 703–706, 1993.

Ohara, T., Akimoto, H., Kurokawa, J., Horii, N., Yamaji, K., Yan, X., and Hayasaka, T.: An Asian emission inventory of anthropogenic emission sources for the period 1980–2020, Atmos. Chem. Phys., 7, 4419–4444, doi:10.5194/acp-7-4419-2007, 2007.

Pacala, S. W., Breidenich, C., Brewer, P. G., Fung, I. Y., Gunson, M. R., Heddle, G., Law, B. E., Marland, G., Paustian, K., Prather, M., Randerson, J. T., Tans, P. P., and Wofsy, S. C.: Verifying greenhouse gas emissions: Methods to support international climate agreements, Committee on Methods for Estimating Greenhouse Gas Emissions; National Research Council, 2010.

Parrish, D. D.: Critical evaluation of US on-road vehicle emission inventories, Atmos. Environ., 40, 2288–2300, 2006.

Peylin, P., Houweling, S., Krol, M. C., Karstens, U., Rödenbeck, C., Geels, C., Vermeulen, A., Badawy, B., Aulagnier, C., Pregger, T., Delage, F., Pieterse, G., Ciais, P., and Heimann, M.: Importance of fossil fuel emission uncertainties over Europe for CO_2 modeling: model intercomparison, Atmos. Chem. Phys. Discuss., 9, 7457–7503, doi:10.5194/acpd-9-7457-2009, 2009.

Potosnak, M. J., Wofsy, S. C., Denning, A. S., Conway, T. J., Munger, J. W., and Barnes, D. H.: Influence of biotic exchange and combustion sources on atmospheric CO_2 concentrations in New England from observations at a forest flux tower, J. Geophys. Res., 104, 9561–9569, 1999.

Pozzer, A., Pollmann, J., Taraborrelli, D., Jöckel, P., Helmig, D., Tans, P., Hueber, J., and Lelieveld, J.: Observed and simulated global distribution and budget of atmospheric C_2-C_5 alkanes, Atmos. Chem. Phys., 10, 4403–4422, doi:10.5194/acp-10-4403-2010, 2010.

Press, W. H. and Teukolsky, S.: Fitting straight line data with errors in both coordinates, Comput. Phys., 6, 274–276, 1992.

Rivier, L., Ciais, P., Hauglustaine, D., Bakwin, P. S., Bousquet, P., Peylin, P., and Klonecki, A.: Evaluation of SF_6, C_2Cl_4 and CO as surrogate tracers for fossil fuel CO_2 in the Northern Hemisphere using a chemistry transport model, J. Geophys. Res., 111, D16311, doi:10.1029/2005JD006725, 2006.

Ryerson, T. B., Trainer, M., Holloway, J., Parrish, D. D., Huey, L., Sueper, D., Frost, G. J., Donnelly, S., Schauffler, S., Atlas, E., Kuster, W., Golden, P., Hubler, G., Meagher, J., and Fehsenfeld, F.: Observations of ozone formation in power plant plumes and implications for ozone control strategies, Science, 292, 719–723, 2001.

Spivakovsky, C. M., Logan, J. A., Montzka, S. A., Balkanski, Y. J., Foreman-Fowler, M., Jones, D., Horowitz, L., Fusco, A., Brenninkmeijer, C. A. M., Prather, M. J., Wofsy, S. C., and McElroy, M. B.: Three-dimensional climatological distribution of tropospheric OH: Update and evaluation, J. Geophys. Res., 105, 8931–8980, 2000.

Stephens, B. B., Gurney, K. R., Tans, P. P., Sweeney, C., Peters, W., Bruhwiler, L., Ciais, P., Ramonet, M., Bousquet, P., Nakazawa, T., Aoki, S., Machida, T., Inoue, G., Vinnichenko, N., Lloyd, J., Jordan, A., Heimann, M., Shibistowa, O., Langenfelds, R. L., Steele, l. P., Francey, R. J., and Denning, A. S.: Weak northern and strong tropical land carbon uptake from vertical profiles of atmospheric CO_2, Science, 316, 1732–1735, 2007.

TEAP: Task force on emissions discrepancies report, UNEP, Montreal Protocol on substances that deplete the ozone layer, 2006.

Trainer, M., Ridley, B., Buhr, M., Kok, G., Walega, J., Hübler, G., Parrish, D. D., and Fehsenfeld, F.: Regional ozone and urban plumes in the southeastern United States: Birmingham, a case study, J. Geophys. Res., 100, 18823–18834, 1995.

Turnbull, J. C., Miller, J. B., Lehman, S. J., Tans, P. P., Sparks, R. J., and Southon, J. R.: Comparison of $^{14}CO_2$, CO and SF_6 as tracers for determination of recently added fossil fuel CO_2 in the atmosphere and implications for biological CO_2 exchange, Geophys. Res. Lett., 33, L01817, doi:10.1029/2005GL024213, 2006.

Turnbull, J. C., Lehman, S. J., Miller, J. B., Sparks, R. J., Southon, J. R., and Tans, P. P.: A new high precision $^{14}CO_2$ time series for North American continental air, J. Geophys. Res., 112, D11310, doi:10.1029/2006JD008184, 2007.

Turnbull, J. C., Rayner, P. J., Miller, J. B., Naegler, T., Ciais, P., and Cozic, A.: On the use of$^{14}CO_2$ as a tracer for fossil fuel CO_2: quantifying uncertainties using an atmospheric transport model, J. Geophys. Res., 114, D22302, doi:10.1029/2009JD012308, 2009.

Turnbull, J. C., Lehman, S. J., Morgan, S., and Wolak, C.: A new automated extraction system for ^{14}C measurement in atmospheric CO_2, Radiocarbon, 52, 1261–1269, 2010.

USEPA: Current methods used to estimate emissions, 1985-1999, Procedures Document for National Emission Inventory, Criteria Air Pollutants 1985–1999, USEPA, 2001.

USEPA: AP-42, Fifth Edition. Compilation of air pollutant emission factors, Volume 1: Point and area sources, USEPA (United States Environmental Protection Agency), Research Triangle Park, NC, 2009.

Vaughn, B. H., Ferretti, D. F., Miller, J. B., and White, J. W. C.: Stable isotope measurements of atmospheric CO_2 and CH_4, in: Handbook of stable isotope analytical techniques, Elsevier BV, Amsterdam, The Netherlands, 2004.

Vogel, F. R., Hammer, S., Steinhof, A., Kromer, B., and Levin, I.: Implication of weekly and diurnal 14C calibration on hourly estimates of CO-based fossil fuel CO_2 at a moderately polluted site in south-western Germany, Tellus, 62, 512–520, doi:10.1111/j.1600-0889.2010.00477.x, 2010.

Warneke, C., de Gouw, J., Stohl, A., Cooper, O., Goldan, P., Kuster, W., Holloway, J., Williams, E., Lerner, B., McKeen, S. A., Trainer, M., Fehsenfeld, F., Altas, E. L., Donnelly, S., Stroud, V., Lueb, A., and Kato, S.: Biomass burning and anthropogenic sources of CO over New England in the summer 2004, J. Geophys. Res., 111, D23S15, doi:10.1029/2005JD006878, 2006.

Warneke, C., McKeen, S. A., de Gouw, J., Goldan, P., Kuster, W., Holloway, J., Williams, E., Lerner, B., Parrish, D. D., Trainer, M., Fehsenfeld, F., Kato, S., Atlas, E. L., Baker, A., and Blake, D. R.: Determination of urban volatile organic compound emission ratios and comparison with an emissions database, J. Geophys. Res., 112, D10S47, doi:10.1029/2006JD007930, 2007.

Watson, J. G., Chow, J. C., and Fujita, E. M.: Review of volatile organic compound source apportionment by chemical mass balance, Atmos. Environ., 35, 1567–1584, 2001.

White, W., Anderson, J., Blumenthal, D., Husar, R., Gillani, N., Husar, J., and Wilson Jr., W.,: Formation and transport of secondary air pollutants: Ozone and aerosols in the St Louis urban plume, Science, 194, 187–189, 1976.

Wofsy, S. C., Fan, S.-M., Blake, D., Bradshaw, J., Sandholm, S., Singh, H., Sachse, G., and Harriss, R.: Factors influencing atmospheric composition over subarctic North America during summer, J. Geophys. Res., 99, 1887–0897, 1994.

Zhao, C. and Tans, P. P.: Estimating uncertainty of the WMO mole fraction scale for carbon dioxide in air, J. Geophys. Res., 111, D08S09, doi:10.1029/2005JD006003, 2006.

Zhao, C., Andrews, A. E., Bianco, L., Eluszkiewicz, J., Hirsch, A., MacDonald, C., Nehrkorn, T., and Fischer, M. L.: Atmospheric inverse estimates of methane emissions from Central California, J. Geophys. Res., 114, 16302, doi:10.1029/2008JD011671, 2009.